Regulation of protein function by native metastability

Cheolju Lee*, Soon-Ho Park, Min-Youn Lee, and Myeong-Hee Yu†

National Creative Research Initiative Center, Korea Research Institute of Bioscience and Biotechnology, 52 Oun-dong, Yusong, Taejon 305-333, Korea

Communicated by Peter S. Kim, Massachusetts Institute of Technology, Cambridge, MA, May 15, 2000 (received for review November 3, 1999)

In common globular proteins, the native form is in its most stable state. In contrast, each native form exists in a metastable state in inhibitory serpins (serine protease inhibitors) and some viral membrane fusion proteins. Metastability in these proteins is critical to their biological functions. Mutational analyses and structural examination have previously revealed unusual interactions, such as side-chain overpacking, buried polar groups, and cavities as the structural basis of the native metastability. However, the mechanism by which these structural defects regulate protein functions has not been elucidated. We report here characterization of cavity-filling mutations of α_1-antitrypsin, a prototype serpin. Conformational stability of the molecule increased linearly with the van der Waals volume of the side chains. Increasing conformational stability is correlated with decreasing inhibitory activity. Moreover, the activity loss appears to correlate with the decrease in the rate of the conformational switch during complex formation with a target protease. These results strongly suggest that the native metastability of proteins is indeed a structural design that regulates protein functions.

The native forms of most proteins are thermodynamically the most stable state (1). However, the native forms of some proteins are metastable: typical examples are the strained native structure of plasma serpins (serine protease inhibitors) (2), the spring-loaded structure of the membrane fusion protein of influenza virus (3, 4), heat shock transcription factors (5), and possibly the surface glycoprotein of human immunodeficiency virus (HIV) (6). Metastability in these proteins is considered to be an important mechanism for regulating their biological functions (2–8). The native strain of serpins is crucial to their physiological function, such as protease inhibition (2, 7), hormone delivery (9), Alzheimer filament assembly (10), and extracellular matrix remodeling (11). The inhibitory serpins include α_1-antitrypsin (α_1AT), α_1-antichymotrypsin, antithrombin-III, plasminogen activator inhibitor-1, C1-inhibitor, and antiplasmin, which regulate processes such as inflammation, coagulation, fibrinolysis, and complement activation (2). The serpin structure is composed of three β-sheets and several α-helices, and the reactive center loop is exposed at one end of the molecule for protease binding (Fig. 1). Upon binding a target protease, the reactive center loop of inhibitory serpins is thought to be inserted into the major β-sheet, A sheet, to form a very stable complex between the inhibitor and the protease (12). Because the metastable native form has an advantage of facile conversion into an alternative more stable conformation, it is conceivable that the native metastability of serpins is used for the facile conformational change during the complex formation.

To understand the structural basis and functional role of the native metastability, we have characterized stabilizing amino acid substitutions of α_1AT, a prototype inhibitory serpin (13–16). Mutational patterns and structural examination of the mutation sites revealed various unusual interactions, such as unusual packing of the side chains in the interior of protein, buried polar groups, and cavities, as the structural basis of native metastability in α_1AT (13–17). Because the inhibitory function of α_1AT was affected by the stabilizing substitutions in the loop insertion region (15) but not by the stabilizing substitutions at the hydrophobic core (13, 14), local stability rather than global stability appears to be critical for regulating inhibitory function. Cavities and unfavorable polar–nonpolar interactions were also found in the crystal structures of both mature and precursor forms of hemagglutinin, the membrane fusion protein of influenza virus (4, 18). These structural defects are likely to be the design principles of the metastable native proteins to regulate their functions. However, the mechanism of how these structural defects regulate the protein functions has yet to be elucidated. In the present study, we characterized a series of cavity-filling mutations of α_1AT that increased the conformational stability gradually. The results show that the native metastability regulates the inhibitory function of α_1AT by controlling the rate of the conformational switch during complex formation with a target protease.

Materials and Methods

Materials. The plasmids for α_1AT expression in *Escherichia coli* and the preparation of recombinant proteins were described previously (13–15). Mutations were introduced by oligonucleotide-directed mutagenesis. Ultrapure guanidinium chloride (GdmCl) was purchased from ICN Biochemicals. Porcine pancreatic elastase (PPE) and *N*-succinyl-$(Ala)_3$-*p*-nitroanilide were purchased from Sigma. *N*,*N*′-dimethyl-*N*-(acetyl)-*N*′-(7-nitrobenz-2-oxa-1,3-diazol-4-yl)ethylenediamine (NBD) was from Molecular Probes. All other reagents were of analytical grade.

Equilibrium Unfolding of α_1AT Variants. Equilibrium unfolding was monitored by spectrofluorimetry (λ_{ex} = 280 nm, λ_{em} = 360 nm) in the presence of GdmCl. The native protein was incubated in a buffer (10 mM phosphate, pH 6.5/50 mM NaCl/1 mM EDTA) containing various concentrations of GdmCl at 25°C for about 4 h before spectral measurements. The concentration of protein was 5 μg/ml. Equilibrium unfolding was fitted to a two-state model as described previously (13–15).

Inhibitory Parameters of α_1AT Variants. The stoichiometry of inhibition (SI) and the association rate of α_1AT variants with PPE were measured. The SI values were determined as described (15). Various amounts of α_1AT variants were incubated with 100 nM PPE in 30 mM sodium phosphate, pH 7.4/160 mM NaCl/0.1% PEG 6000/0.1% Triton X-100. After incubation at 37°C for 10 min, the reaction mixture was diluted 10-fold with the same buffer and the residual protease activity was determined by using *N*-succinyl-$(Ala)_3$-*p*-nitoranilide as a substrate. Linear regression analysis of the decrease in proteinase activity with increasing molar ratio of α_1AT to PPE yielded the estimate for the SI as the intercept on the abscissa. The association rate constant for α_1AT with PPE was determined by use of a continuous assay

Abbreviations: serpin, serine protease inhibitor; α_1AT, α_1-antitrypsin; GdmCl, guanidinium chloride; SI, stoichiometry of inhibition; PPE, porcine pancreatic elastase; NBD, *N*,*N*′-dimethyl-*N*-(acetyl)-*N*′-(7-nitrobenz-2-oxa-1,3-diazol-4-yl)ethylenediamine.

*Present address: BMBCB, Northwestern University, 2153 N. Campus Dr., Evanston, IL 60208.

†To whom reprint requests should be addressed. E-mail: mhyu@mail.kribb.re.kr.

The publication costs of this article were defrayed in part by page charge payment. This article must therefore be hereby marked "*advertisement*" in accordance with 18 U.S.C. §1734 solely to indicate this fact.

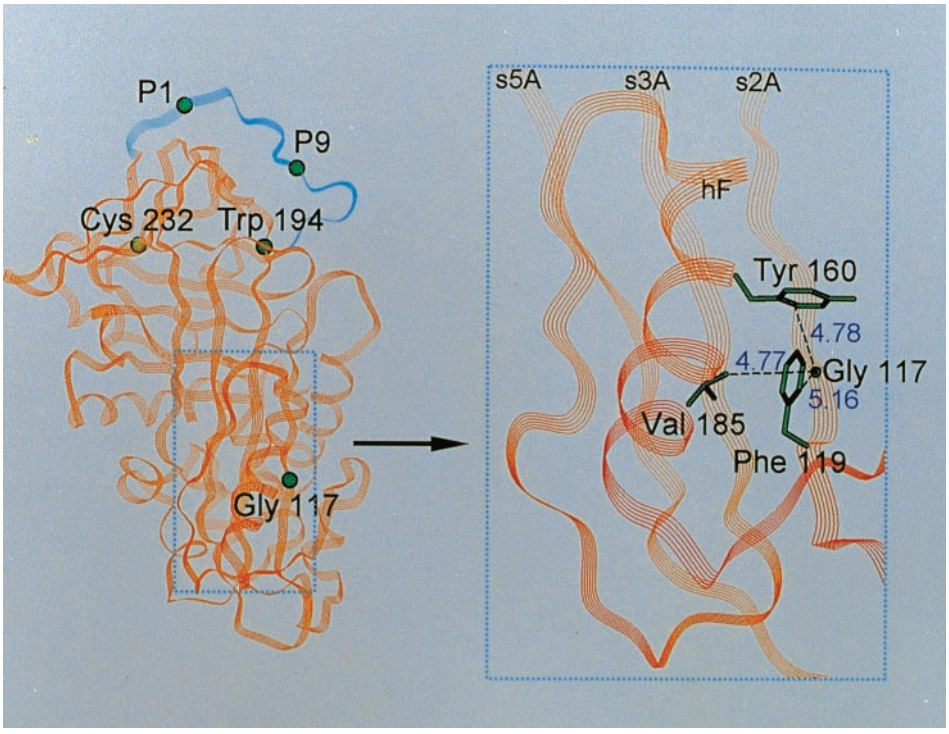

Fig. 1. (*Left*) Schematic drawing of the structure of α_1-AT and the cavity interactions near Gly-117. The designation of secondary structures of ref. 2 was followed. The reactive center loop, which is inserted into β-sheet A as the fourth strand upon cleavage by target protease, is colored in cyan. P1 and P9 are the first and ninth residues amino-terminal of the scissile bond. (*Right*) C^{α} of Gly-117 and the side chains of neighboring residues are shown in a close-up view. Interatomic distances are designated in Å and straight dotted lines. The diagram was produced by using INSIGHTII (Molecular Simulations, San Diego).

procedure (19, 20). PPE (3 nM) was incubated with various concentrations of α_1AT (20 to ≈125 nM) in the presence of 1 mM *N*-succinyl-$(Ala)_3$-*p*-nitroanilide in 30 mM sodium phosphate, pH 7.4/160 mM NaCl/0.1% PEG 6000/0.1% Triton X-100. The reaction was continuously recorded at 410 nm.

Stopped-Flow Measurement of Conformational Switch. Time-resolved fluorescence change was measured with an SFM-4 stopped-flow apparatus (Bio-Logic, Claix, France). Experiments were carried out in 10 mM sodium phosphate, pH 6.5/50 mM NaCl/1 mM EDTA at 25°C. For the reaction of NBD-labeled α_1AT and PPE, NBD probe was attached to the P9 position of the reactive center loop (Fig. 1; ref. 21). To introduce the probe at a unique site, the original single cysteine at position 232 (Fig. 1) was replaced with serine, then alanine at P9 (Ala-350) was replaced with cysteine. This mutant showed virtually identical inhibitory activity compared with the wild-type α_1AT. Three α_1AT variants at position 117 (Val, Ile, and Phe) in NBD labeling were constructed with the same background of C232S/A350C. Reactions were carried out at a final concentration of 60 nM NBD-α_1AT and at various concentrations of PPE. The fluorescence of NBD was excited at 480 nm, and the change in fluorescence above 495 nm was measured by using a filter with a 495-nm cut-off.

Results and Discussion

Cavities as a Structural Basis of the Native Metastability. In the native structure of α_1AT (16), C^{α} of Gly-117 is surrounded by Phe-119, Tyr-160, and Val-185 on the outer face of β-sheet A (Fig. 1 *Right*). The site, initially identified by a thermostable mutation (G117V: replacement of Gly-117 by Val) in screening, appears to form a cavity having the nearest side-chain carbon atoms 4.8 Å apart. Cavities are a source of energetic cost in protein stability (22). We measured this cost by constructing several mutants of α_1AT in which the Gly-117 residue was replaced with a series of other hydrophobic amino acids. The conformational stability of α_1AT variants was measured in GdmCl-induced equilibrium unfolding by monitoring the changes in intrinsic tryptophan fluorescence (Fig. 2). The plot of changes in the stabilization energy ($\Delta\Delta G$) as a function of the change in the van der Waals volume of the residue (23) is linear with a slope of 35 $cal \cdot mol^{-1} \cdot Å^{-3}$ (Fig. 3). This value, equivalent to 0.87 $kcal \cdot mol^{-1}$ contribution per methylene group, is comparable to the values obtained by cavity-filling mutations in RNase HI (24) or by cavity-creating mutations in T4 lysozyme (22) and chymotrypsin inhibitor 2 (25). The results indicate that the site near Gly-117 indeed forms a cavity that can accommodate much larger side chains without significantly altering the main structure. It is likely that the cavity near Gly-117 contributes to the native metastability of α_1AT.

Inverse Correlation Between Conformational Stability and Inhibitory Activity. The inhibition process of serpins can be described as a suicide substrate mechanism (26), in which serpins, upon binding with proteases, partition between cleaved serpins and stable serpin-enzyme complexes as described in Scheme 1.

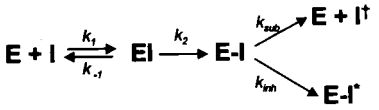

Scheme 1.

In this scheme, I denotes the serpin; E, protease; EI, noncovalent Michaelis complex; E-I, a proposed intermediate before partitioning; E-I*, stable enzyme-inhibitor complex; and $I^{\dagger}$, cleaved serpin. The outcome of a given serpin–protease interaction, therefore, depends on the partitioning ratio between the inhib-

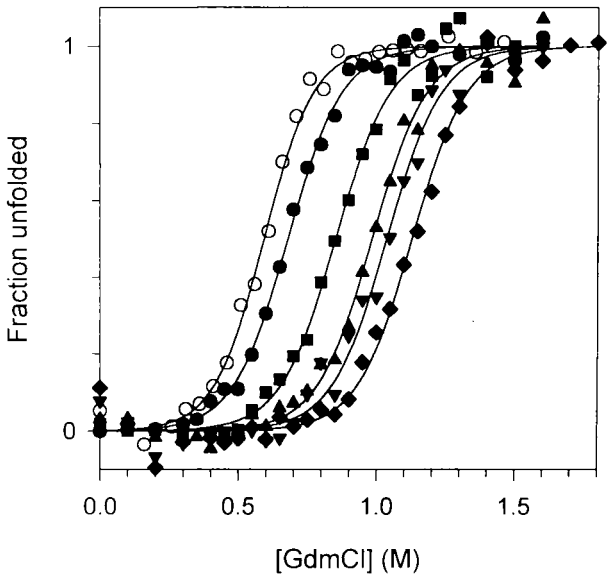

Fig. 2. GdmCl-induced equilibrium unfolding transition of mutant α_1AT. Equilibrium unfolding of α_1AT was monitored by fluorescence spectroscopy with excitation at 280 nm and emission at 360 nm. Native α_1AT was diluted into an appropriate GdmCl solution and incubated at 25°C for 4 h. The buffer was 10 mM sodium phosphate/50 mM NaCl/1 mM EDTA, pH 6.5, and the final protein concentration was 5 μg/ml. ○, wild type; ●, G117A; ■, G117V; ▲, G117L; ▼, G117I; ◆, G117F.

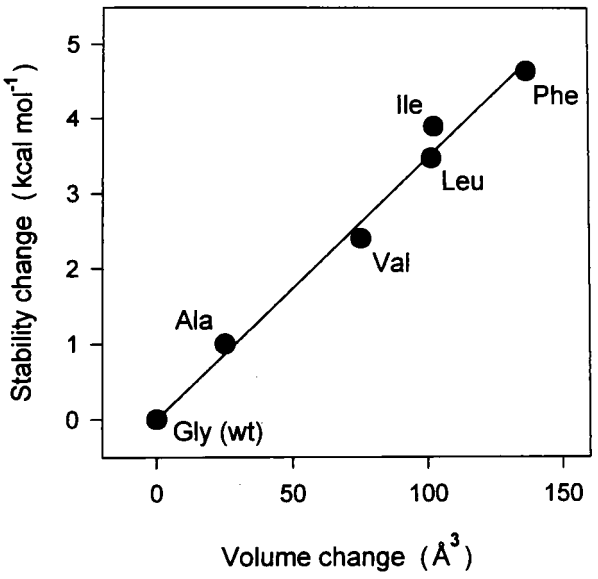

Fig. 3. Effect of amino acid substitutions for Gly-117 on the stability of α_1AT. Changes in free energy of stabilization ($\Delta\Delta G$) as a function of the increase in van der Waals volume of the side chain are plotted. The difference in stabilization between the mutant and the wild-type α_1AT was calculated from $\Delta\Delta G = \Delta C_m \times 7.9$ kcal·mol^{-1}·M^{-1} (average m value: denaturant-dependent free energy change) where ΔC_m is the difference between the concentration at the transition midpoint of the wild-type and that of mutant α_1AT measured by equilibrium unfolding experiments as in Fig. 2. Each label is the three-letter code for the amino acid substituted at the 117 site, and wt indicates wild-type protein. The line through the data points was obtained by least-squares fit.

itory (k_{inh}) and substrate (k_{sub}) pathways, which is represented by the stoichiometry of inhibition (SI = 1 + k_{sub}/k_{inh}; good inhibitors have the value of 1 because most of the serpin molecules partition into complex formation and k_{sub}/k_{inh} is close to 0; ref. 20). To understand effect of the stabilizing mutations of α_1AT on the inhibitory activity, we measured SI values of each α_1AT variant against PPE as well as association rate constants (k_{app}). All of the mutations increased SI values but did not affect the association rate (Table 1). This finding indicates that the mutations at Gly-117 did not influence initial protease binding but did affect a later step, probably the partitioning point during complex formation (20). Strikingly, the increase in SI values correlates strongly with increases in the stability of α_1AT (Fig. 4). Moreover, an additional mutation of Y160A in G117F background partially restored the inhibitory activity at the cost of conformational stability (square in Fig. 4). These results clearly establish an inverse correlation between the conformational stability and the inhibitory activity of α_1AT: an increase in the conformational stability is detrimental to the protein function.

Retardation of Loop Insertion by Cavity-Filling Mutations. Complex formation of a serpin with its target protease accompanies a massive conformational change in the serpin molecules: the reactive center loop is inserted into β-sheet A as the fourth strand, while the protease is covalently linked to the reactive center loop as an acyl intermediate (12, 27, 28). To probe the loop insertion process during the complex formation, we introduced cysteinyl residue at the P9 position (ninth residue amino-terminal from the scissile bond; Fig. 1) of the reactive center loop, and labeled it with a fluorescent probe, NBD (21). The NBD labeling did not alter the inhibitory activity significantly (Table 1). We measured how fast the probe moves into a hydrophobic environment by measuring the rate of NBD fluorescence increase when α_1AT binds to PPE. The change of NBD fluorescence was measured under pseudo-first-order reaction conditions by rapid mixing of NBD-labeled α_1AT with increasing amounts of PPE by using stopped-flow fluorimetry. Fig. 5*A* shows representative progress curves for the wild-type α_1AT. All of the progress curves exhibited single-exponential phases that are extrapolated to the fluorescence of free α_1AT at zero time. This observation indicates that the association of PPE with α_1AT did not alter the fluorescence properties of NBD attached at the P9 position, hence the observed increase in fluorescence reflects the loop insertion. The observed rate constants (k_{obs}) increased with increasing PPE concentrations (Fig. 5*B*), and the limiting rate constants of NBD fluorescence change were obtained by fitting the plot of k_{obs} vs. [PPE] to a hyperbolic equation (Table

Table 1. Inhibitory parameters and conformational switch rate of α_1AT variants

Residue 117	SI*	k_{app},† 10^5 M^{-1}·s^{-1}	SI_{NBD}‡	k_{obs},§ s^{-1}
Gly (wt)	1.66 ± 0.06	3.86 ± 0.26	1.71 ± 0.05	2.05
Ala	1.70 ± 0.03	4.10 ± 0.41	ND	ND
Val	1.91 ± 0.05	3.85 ± 0.26	1.85 ± 0.07	2.00
Leu	2.21 ± 0.09	4.07 ± 0.21	ND	ND
Ile	2.50 ± 0.08	4.20 ± 0.23	2.49 ± 0.08	1.93
Phe	3.99 ± 0.12	4.80 ± 0.38	3.60 ± 0.21	1.65

ND, not determined; wt, wild type.

*The number of moles of α_1AT required to completely inhibit 1 mole of PPE.

†Apparent second-order association rate constant of α_1AT with PPE, which corresponds to k_1k_2/k_{-1} in Scheme 1 (20).

‡Stoichiometry of inhibition of the NBD-labeled α_1AT variants carrying C232S and A350C mutations.

§Pseudo-first-order rates for the increase in NBD fluorescence. The values are the limiting rates obtained by fitting the measured rates at various concentrations of PPE to a hyperbolic function.

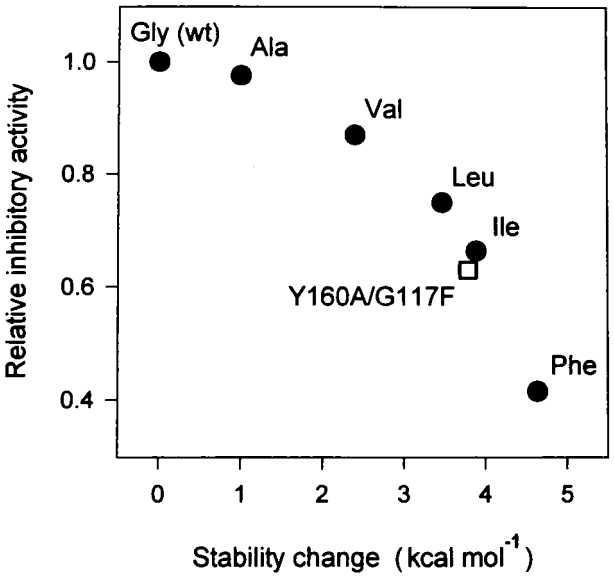

Fig. 4. Inverse correlation between the conformational stability and the inhibitory activity of α_1AT variants. Relative inhibitory activity is indicated as the ratio of SI value for the wild-type to that of mutant α_1AT. □ indicates the double substitution, Y160A/G117F.

1). The rate of NBD fluorescence change for the wild-type α_1AT was 2.05 s^{-1}, and it decreased gradually as the protein stability increased (≈20% decrease for G117F). The results indicate that increasing the conformational stability of α_1AT retards the docking of the P9 position of the reactive center loop into the main body of the molecule.

Implications for the Inhibitory Mechanism. It was thought that the relative magnitudes of the rate constants of individual pathways after the branch point in the inhibitory mechanism, k_{sub} and k_{inh}, are controlled by hydrolysis of the acyl enzyme intermediate and the formation of protease-inhibitor complex, respectively (12, 20). We could not determine directly the mutational effects on the changes in the individual rate constants. The simplest interpretation is that the mutations specifically affected the rate of complex formation (k_{inh}) and that k_{sub} is an aqueous deacylation rate that was not affected by the mutations. Our results, however, showed that the magnitude of the changes in the rate of loop insertion is not as great as that in SI values (Table 1). The results imply that retardation of the loop insertion may perturb both of the rates, k_{sub} and k_{inh}, in opposite directions, and that k_{sub} in Scheme 1 may not be merely an aqueous deacylation. Recent reports also suggested that k_{sub} is not a simple aqueous deacylation rate but a compound rate that accounts for the displacement of the reactive center loop from the protease (29). It is also possible that a small structural change at the mutation site enhanced the rate of the deacylation. However, the Gly-117 site lies between helix F and β-sheet A (Fig. 1), far away from the initial protease-binding site, and not the small structural change *per se* but the change in conformational property is likely to influence the deacylation. It is likely that stabilization by the mutations specifically affected the rate of complex formation (k_{inh}) by retarding the loop insertion, and that retardation of the loop insertion allows more of the molecules available for deacylation, resulting in an enhancement in k_{sub}. The cavity around Gly-117 may exist to destabilize the native interactions between helix F and the β-sheet A for a facile conformational change during complex formation with a target protease. Cavity-filling at the site of residue 117 may increase the activation energy

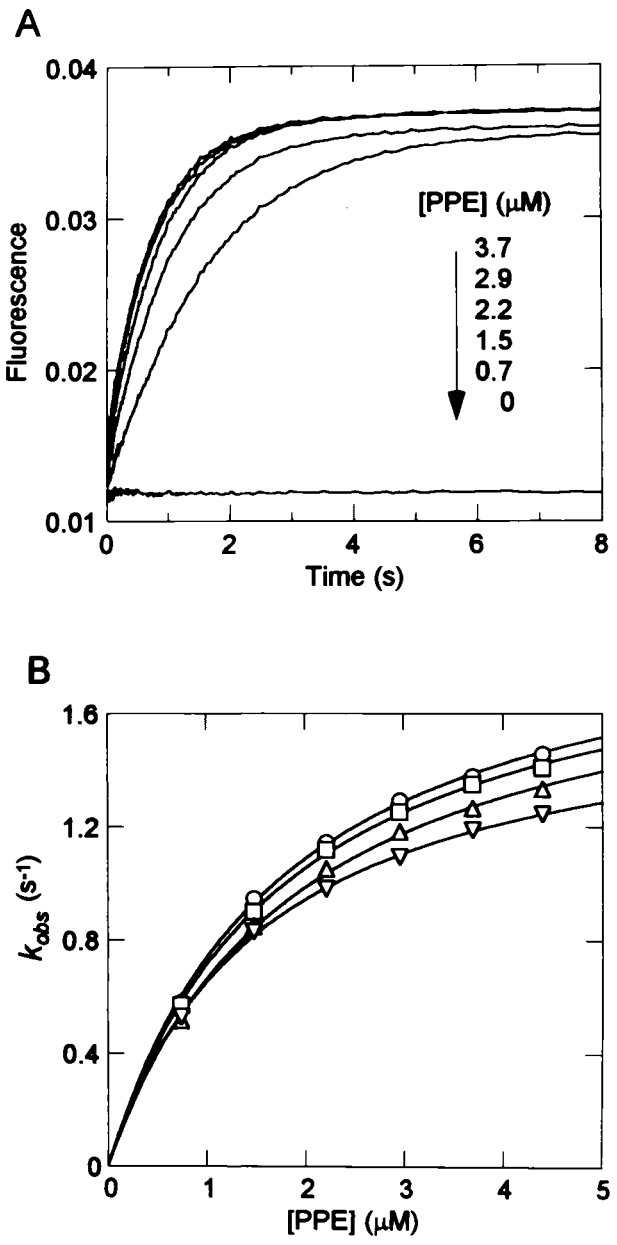

Fig. 5. Stopped-flow fluorescence measurement of NBD fluorescence change. (*A*) Kinetic traces of the pseudo-first-order reaction of NBD-labeled wild-type α_1AT with increasing concentrations of PPE. (*B*) The observed rate constants at various PPE concentrations for the variant α_1AT carrying stabilizing substitutions at residue 117. ○, wild type; □, G117V; △, G117I; ▽, G117F. The lines represent hyperbolic fits obtained by nonlinear least-squares analysis.

barrier for the loop insertion, mainly by providing more favorable native interactions in β-sheet A and helix F. Our results suggest that the loss of inhibitory activity, which shows a correlation with the stability increase, is due to reduction in the rate of conformational switch during the complex formation.

Biological Significance. The results of the present study strongly suggest that the native form of inhibitory serpins has evolved as a poorly folded structure that enables sophisticated regulation of protease inhibition. Perhaps the conformational switch is driven by mobilization of unfavorable interactions in the native state

into more favorable ones. Unfavorable interactions appear to control conformational switch in other proteins. The precursor structure of hemagglutinin, the membrane fusion protein of the influenza virus, features unusual interactions, such as the presence of both cavities and a strained loop in a region where the cleavage induces mature conformation (18). The mature form of hemagglutinin is also metastable (8), with unfavorable interactions such as buried ionizable residues that may serve as an acid-induced conformational switch to form a fusion-active state (4, 17). Cavities found in the metastable procapsid lattice of bacteriophage P22 also appear to play a role in capsid maturation (30). In addition, structural and mutational studies of arrestin, a desensitizer of the signaling of G-protein-coupled receptors, suggest that buried polar networks may trigger conformational switch when binding a phosphorylated form of G-protein-coupled receptor (31, 32). Our results show clearly that the cavity near the Gly-117 site in α_1AT is an energetic cost and plays an essential role for the inhibitory activity.

In conclusion, the native metastability of proteins, seemingly due to folding defects, is indeed a structural design that regulates protein functions, presumably by facilitating conformational switch.

We thank Drs. H. Im and J.-S. Shin for helpful comments. This research was supported by National Creative Research Initiatives grant from the Korean Ministry of Science and Technology.

1. Anfinsen, C. B. (1973) *Science* **181,** 223–230.
2. Huber, R. & Carrell, R. W. (1989) *Biochemistry* **28,** 8951–8966.
3. Carr, C. M. & Kim, P. S. (1993) *Cell* **73,** 823–832.
4. Bullough, P. A., Hughson, F. M., Skehel, J. J. & Wiley, D. C. (1994) *Nature (London)* **371,** 37–43.
5. Orosz, A., Wisniewski, J. & Wu, C. (1996) *Mol. Cell. Biol.* **16,** 7018–7030.
6. Chan, D. C., Fass, D., Berger, J. M. & Kim, P. S. (1997) *Cell* **89,** 263–273.
7. Stein, P. E. & Carrell, R. W. (1995) *Nat. Struct. Biol.* **2,** 96–113.
8. Carr, C. M., Chaudhry, C. & Kim, P. S. (1997) *Proc. Natl. Acad. Sci. USA* **94,** 14306–14313.
9. Pemberton, P. A., Stein, P. E., Pepys, M. B., Potter, J. M. & Carrell, R. W. (1988) *Nature (London)* **336,** 257–258.
10. Ma, J., Yee, A., Brewer, H. B., Jr., Das, S. & Potter, H. (1994) *Nature (London)* **372,** 92–94.
11. Stefansson, S. & Lawrence, D. A. (1996) *Nature (London)* **383,** 441–443.
12. Wright, H. T. & Scarsdale, J. N. (1995) *Proteins Struct. Funct. Genet.* **22,** 210–225.
13. Lee, K. N., Park, S. D. & Yu, M.-H. (1996) *Nat. Struct. Biol.* **3,** 497–500.
14. Lee, K. N., Im, H., Kang, S. W. & Yu, M.-H. (1998) *J. Biol. Chem.* **273,** 2509–2516.
15. Im, H., Seo, E. J. & Yu, M.-H. (1999) *J. Biol. Chem.* **274,** 11072–11077.
16. Ryu, S.-E., Choi, H.-J., Kwon, K.-S., Lee, K. N. & Yu, M.-H. (1996) *Structure* **4,** 1181–1192.
17. Elliott, P. R., Abrahams, J.-P. & Lomas, D. A. (1998) *J. Mol. Biol.* **275,** 419–425.
18. Chen, J., Lee, K. H., Steinhauer, D. A., Stevens, D. J., Skehel, J. J. & Wiley, D. C. (1998) *Cell* **95,** 409–417.
19. Chaillan-Huntington, C. E. & Patston, P. A. (1998) *J. Biol. Chem.* **273,** 4569–4573.
20. Hood, D. B., Huntington, J. A. & Gettins, P. G. W. (1994) *Biochemistry* **33,** 8538–8547.
21. Shore, J. D., Day, D. E., Francis-Chmura, A. M., Verhamme, I., Kvassman, J. Lawrence, D. A. & Ginsburg, D. (1995) *J. Biol. Chem.* **270,** 5395–5398.
22. Eriksson, A. E., Baase, W. A., Zhang, X. J., Heinz, D. W., Blaber, M., Baldwin, E. P. & Matthews, B. W. (1992) *Science* **255,** 178–183.
23. Chothia, C. (1975) *Nature (London)* **254,** 304–308.
24. Akasako, A., Haruki, M., Olbatake, M. & Kanaya, S. (1997) *J. Biol. Chem.* **272,** 18686–18693.
25. Jackson, S. E., Moracci, M. elMasry, N., Johnson, C. M. & Fersht, A. R. (1993) *Biochemistry* **32,** 11259–11269.
26. Patston, P. A., Gettins, P., Beechem, J. & Schapira, M. (1991) *Biochemistry* **30,** 8876–8882.
27. Lawrence, D. A., Ginsburg, D., Day, D. E., Berkenpas, M. B., Verhamme, I. M., Kvassman, J.-O. & Shore, J. D. (1995) *J. Biol. Chem.* **270,** 25309–25312.
28. Wilczynska, M., Fa, M., Karolin, J., Ohlsson, P.-I., Johansson, L. B.-A. & Ny, T. (1997) *Nat. Struct. Biol.* **4,** 354–357.
29. Kvassman, J.-O., Verhamme, I. & Shore, J. D. (1998) *Biochemistry* **37,** 15491–15502.
30. de Sousa, P. C., Jr., Tuma, R., Prevelige, P. E., Jr., Silva, J. L. & Foguel, D. (1996) *J. Mol. Biol.* **287,** 527–538.
31. Hirsch, J. A., Schubert, C., Gurevich, V. V. & Sigler, P. B. (1999) *Cell* **97,** 257–269.
32. Vishnivetskiy, S. A., Paz, C. L., Schubert, C., Hirsch, J. A., Sigler, P. B. & Gurevich, V. V. (1999) *J. Biol. Chem.* **274,** 11451–11454.